Motion Planning Algorithm of a Multi-Joint Snake-Like Robot Based on Improved Serpenoid Curve

DONGFANG LI[ID][1,3]**, CHAO WANG**[ID][2]**, HONGBIN DENG**[ID][1]**, AND YIRAN WEI**[ID][1]
[1]Beijing Institute of Technology, Beijing 100081, China
[2]China North Industries Corp, Beijing 100053, China
[3]Shandong University of Technology, Zibo 255000, China

Corresponding author: Hongbin Deng (denghongbin@bit.edu.cn)

ABSTRACT In order to study the winding motion of a multi-joint snake-like robot with multi-degree of redundancy in plane, a motion planning algorithm of a multi-joint snake-like robot based on improved Serpenoid curve equation is proposed in this paper. Firstly, the kinematics and dynamics models of a multi-joint snake-like robot are established, and the joint angle curve equation and the thrust expression of each joint of the robot relative to time are obtained. Next, the existing Serpenoid curve equation is improved to calculate the axial bending moment function with joint angle amplitude adjustment factor and turn angle adjustment factor. By analyzing the relationship between the forward thrust of the robot and the improved Serpenoid curve equation, a simple, efficient and reliable closed-loop control system was designed. Then, MATLAB and SimWise4D were used for simulation to obtain the motion trajectory of the robot based on the improved Serpenoid curve motion planning algorithm, and the influence of different parameters on the forward velocity of the multi-joint snake robot was analyzed. Finally, the validity of the motion planning algorithm of a multi-joint snake-like robot based on improved Serpenoid curve equation is verified by the actual experiment.

INDEX TERMS Multi-joint snake-like robot, serpenoid curve, axial bending moment, closed-loop control.

I. INTRODUCTION

The study of multi-joint snake-like robots involves bionics, dynamics, control theory and multi-sensor technology. The robot has high flexibility, super convenience and redundancy. The robot can not only accomplish important tasks such as earthquake relief, fire extinguishing and war investigation in engineering, but provide experimental platform for people to study artificial intelligence, control theory and mechanical analysis in experiments [1], [2]. Therefore, the research of a multi-joint snake-like robot has important engineering application value and strategic significance [3], [4].

The most common motion mode to study multi-joint snake-like robots is winding motion, which is very similar to the sine function. The phase and amplitude in the motion equation change with time [5]. At present, the research on the gait of a multi-joint snake-like robot mainly focuses

on two-dimensional gait and three-dimensional gait. In the research of two-dimensional gait of a multi-joint snake-like robot, Gary is the first researcher who put forward the snake-like motion analysis method. He believes that the biological snake needs a vertical normal force in the course of its movements, by which the snake body generates forward motion [6]. Professor Shigeo Hirose analyzed the movement and skeleton distribution of a snake in detail. He proposed the Serpenoid curve equation of a snake shaped winding motion, established the dynamic link model of a snake-like robot, and obtained the mathematical expression of a snake like winding motion [7]. But the Serpenoid curve equation is two-dimensional, which cannot explain the three-dimensional motions of a multi-joint snake-like robot. Professor Diana Rincon of Florida International University analyzed the winding movement gait of a multi-joint snake-like robot based on the link model, and he established the kinematics link model and the dynamic link model of the robot [8]. However, he did not analyze and validate the model of his robot from

the aspects of simulation and reality. Professor Scott Kelly and Jim Ostrowski of California Institute of Technology set up a dynamic model for a multi-joint snake-like robot with only 3 driven wheels, and they then carried out controllability analysis. However, there were only 3 moving wheels in each joint of the robot, which caused the movement of the robot to be severely restricted by the environment [9]. Professor Pal Liljeback of Norwegian University of Science and Technology analyzed the relationship between a multi-joint snake-like robot and its obstacles in the course of the robot's movement. They proposed the obstacle avoidance assisted movement gait of the robot, which improved the adaptability of the robot to complicated environment [10]. Shugen Ma, a professor at the Shenyang Institute of Automation, Chinese Academy of Sciences, has updated the Serpenoid curve equation of the winding motion of a snake [11]. He proposed the Serpentine curve method to improve the movement efficiency of the multi-joint snake-like robot [12]–[14]. Professor Diana Rincon of Florida International University analyzed a crawling gait of a snake-like robot based on four links. A kinematics model and a dynamic model of a four link robot were established. This model is simple in modeling and is easy to calculate, but it is often restricted by geographical environment in experiments because of its limited joint. [8]. Matsuno et al. analyzed the winding gait of a robot based on the two-dimensional meandering gait of the snake-like robot, and proposed a three-dimensional dynamic model of the snake-like robot with multi-link components [15], [16]. In this model, the multi-joint snake-like robot is composed of a link joint component and a head component that can be lifted, but the link component only shows the ground friction characteristics similar to a real snake, and the robot cannot achieve lateral movement [15], [17], [18]. Professor Ross L. Hatton of Carnegie Mellon University has proposed a snake-like helical method to achieve the helical movement of a multi-joint snake robot on the ground [19]. Shigeo Hirose of Tokyo Institute of Technology proposed the arc link structure of a multi-joint snake-like robot. He established the arc link model, and realized the smooth movement of a robot in space [7], [20].

In the field of motion control of snake-like robots, Alireza Mohammadi et al. studied the path tracking control of the snake-like robot. They designed a constraint function to control the rotation angle and forward velocity of the robot head [21]. Ehsan rezapour et al. of Norwegian University of science used a virtual integrity constraint to study the path tracking control of the snake-like robot. They designed a linear feedback control law to make the robot successfully converge to the set path [22], [23].

Because the basic principles of motion planning for a multi-joint snake-like robot are contained in a two-dimensional plane. Therefore, many achievements have been made in the research of the kinematics and dynamic models of the robot's two-dimensional gait. The motion of the multi-joint snake-like robot also exists in the two-dimensional plane. The study of the two-dimensional gait of a robot can

lay a solid theoretical foundation for the study of the three-dimensional gait of a robot [24], [25].

In this paper, a motion planning algorithm of a wheeled multi-joint snake-like robot with non-holomorphic constraint based on improved Serpenoid curve equation is proposed to realize the winding and sideslip motion of the robot in plane. This method is based on the two-dimensional motion plane of a multi-joint snake-like robot [9], [26]. A robot with non-holonomic constraint allows dimensions of its actuator to be less than the number of generalized coordinates in the system. Such a robot can reduce the weight of the system, improve the operating velocity of the system, reduce the cost of the system and reduce the failure rate of the system. Therefore, it is of great significance to study the motion planning algorithm of a wheeled multi-joint snake-like robot with non-holonomic constraints. Firstly, according to the self-structure and joint characteristics of a multi-joint snake-like robot, the kinematics link model of a multi-joint snake-like robot is established. The link of this model does not deform. The rotation angle between the link and the link can be generated to control the rotation of the robot's link. Kinematics analysis of a multi-joint snake-like robot is carried out, and the joint angle curve equation relative to time variation is obtained, which greatly simplifies the computational efficiency of motion control algorithm. Next, the dynamic model of a multi-joint snake-like robot is established, and the dynamic characteristics between the motion velocity and friction of the link joint are analyzed. The torque balance equation of the link joint is deduced, and the thrust expression of each joint of a multi-joint snake-like robot is obtained. This thrust expression effectively establishes the relationship between the joint motion mode, velocity and angular velocity of the robot. Then, the Serpenoid curve equation of a multi-joint snake-like robot is improved by adding a joint angle amplitude adjustment factor and a turning angle adjustment factor relative to time variation. The axial bending moment equation of a multi-joint snake-like robot with adjusting amplitude and turning angles is obtained. The equation is the improved Serpenoid curve equation. The equation establishes the relationship between the position of each joint and the swing amplitude of the robot, which makes the amplitude of each joint change with time at different positions of the robot. The axial bending moment at the tail provides the forward power for the robot. Finally, the dynamic of the improved Serpenoid curve equation was analyzed, and a closed-loop control system was designed to control the forward motion of the robot [27].

In fact, the main innovations of this paper are as follows: (1) The Serpenoid curve equation is improved to obtain the axial bending moment function of the multi-joint snake-like robot with amplitude adjustment factor and a turning angles adjustment factor, so that the amplitude of the robot joints varies with time at different positions. (2) This paper analyzes the relationship between the forward thrust of the multi-joint snake-like robot and the improved Serpenoid curve equation, and designs a closed-loop control system, which enables

the multi-joint Serpenoid robot to obtain simple, efficient and reliable joint angles and feedback velocity during the movement.

In order to verify the effectiveness of the multi-joint snake robot motion planning algorithm based on the improved Serpenoid curve equation, the proposed control algorithm is simulated by MATLAB. By observing the motion mode of the multi-joint snake-like robot, the trajectory of the robot is analyzed, and the simulation effectiveness of the algorithm is verified. Next, according to the structure characteristics and motion mechanism of the multi-joint snake-like robot, the real structure model of the robot is established. After that, the dynamic simulation of the multi-joint snake-like robot is carried out by using SimWise4D multi-entity dynamic simulation software. The relative joint angle input curve, snake tail displacement curve, snake tail velocity curve, driven wheel rotation curve, contact force of driven wheel and friction force of driven wheel are analyzed based on improved Serpenoid curve motion planning algorithm. The effects of the swing amplitude, frequency of the swing periodic and the moving phase between adjacent links on the forward velocity of the multi-joint snake-like robot is compared, and the effectiveness of the algorithm is verified. Finally, the multi-joint snake-like robot is placed on different pavements for experiment. Each joint of the robot is input into two blocks of control instructions in turn, and the position and velocity of the robot are transformed into a multi-block state feedback form. By analyzing the influences of swing amplitude of the multi-joint snake-like robot on the motion velocity and time of the robot, the effectiveness of the motion planning algorithm of the multi-joint snake-like robot based on improved Serpenoid curve is verified.

The rest of this paper is organized as follows: Section 2 establishes the kinematics model and dynamic model of a multi-joint snake-like robot in detail. Section 3 improves the Serpenoid curve equation according to the kinematics model of the multi-joint snake-like robot. According to the dynamic model of the multi-joint snake-like robot, the relationship between the forward thrust of the robot and the improved Serpenoid curve equation are analyzed. In Section 4, the multi-joint snake-like robot is simulated. Section 5 carries out a prototype experiment on the multi-joint snake-like robot to verify the effectiveness of the motion planning algorithm. Finally, Section 6 draws a conclusion.

II. MODELING OF A MULTI-JOINT SNAKE-LIKE ROBOT
A. KINEMATICS MODEL OF A MULTI-JOINT SNAKE-LIKE ROBOT

The simulation model of a multi-joint snake-like robot consists of N link joints with $2h$ lengths [28]. There are $N-1$ joints between the links, each of which is driven by the joint steering gear [29]. There are driven wheels in the middle of each link [16], [30]. In the link joint of a multi-joint snake-like robot, the widths of each joint and links are not considered. The kinematics model of the robot is shown in Fig. 1.
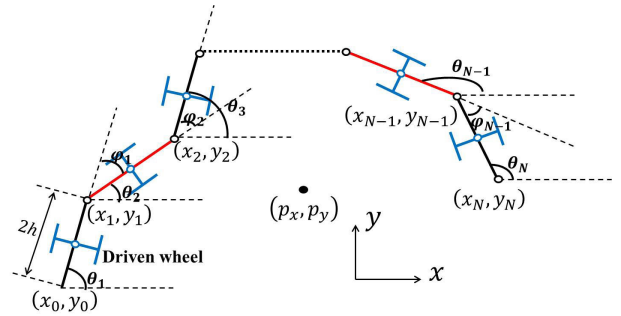

FIGURE 1. Kinematics model of a multi-joint snake-like robot.

The angle of the link at the $j \in \{1, \ldots, N\}$th joint of the multi-joint snake-like robot is θ_j. This angle is the angle between the links and the horizontal direction [31]. The set of angles is the angle of the links $\boldsymbol{\theta} = [\theta_1, \ldots, \theta_N] \in \mathbb{R}^N$. The joint angle at the $j \in \{1, \ldots, N\}$th joint of the robot is $\varphi_j = \theta_j - \theta_{j+1}$, which is the rotation angle between the front and rear links [16], [32]. The set of angles is the joint angle $\boldsymbol{\varphi} = [\varphi_1, \ldots, \varphi_{N-1}] \in \mathbb{R}^{N-1}$. The centroid of each joint of the multi-joint snake-like robot is located at the center of the joint (x_j, y_j), and the coordinates of the links are $\boldsymbol{x} \in \mathbb{R}^N$ and $\boldsymbol{y} \in \mathbb{R}^N$ [29], [33]. The constraint conditions between links satisfy (1).

$$x_j - x_{j-1} = h \cos \theta_j + h \cos \theta_{j-1}$$
$$y_j - y_{j-1} = h \sin \theta_j + h \sin \theta_{j-1} \quad (1)$$

Eq.(1) is superimposed to obtain (2). Where the tail joint is (x_0, y_0), the initial angle of the tail joint is θ_0.

$$\begin{cases} x_j - x_0 = 2h \sum_{i=1}^{j-1} \cos \theta_i + h \cos \theta_j + h \cos \theta_0 \\ y_j - y_0 = 2h \sum_{i=1}^{j-1} \sin \theta_i + h \sin \theta_j + h \sin \theta_0 \end{cases} \quad (2)$$

The position of the head joint is (x_N, y_N), and the constraint condition satisfies (3).

$$\begin{cases} x_N = x_0 + h \cos \theta_0 \\ y_N = y_0 + h \sin \theta_0 \end{cases} \quad (3)$$

Eq.(3) is introduced into (2), and (4) is obtained [29].

$$\begin{cases} x_j = x_N + 2h \sum_{i=1}^{j-1} \cos \theta_i + h \cos \theta_j \\ y_j = y_N + 2h \sum_{i=1}^{j-1} \sin \theta_i + h \sin \theta_j \end{cases} \quad (4)$$

Eq.(4) is differentiated and the velocity equation of the robot link joint is obtained as shown in (5).

$$\begin{cases} \dot{x}_j = \dot{x}_N - 2h \sum_{i=1}^{j-1} \dot{\theta}_i \sin \theta_i - h \dot{\theta}_j \sin \theta_j \\ \dot{y}_j = \dot{y}_N + 2h \sum_{i=1}^{j-1} \dot{\theta}_i \cos \theta_i + h \dot{\theta}_j \cos \theta_j \end{cases} \quad (5)$$

The non-holonomic constraint condition considering that the driven wheel does not slip is shown in (6). the velocity of the head joint is $(\dot{x}_N, \dot{y}_N)$.

$$\dot{x}_j \sin \theta_j = \dot{y}_j \cos \theta_j \quad i = 1, 2, \ldots N \tag{6}$$

Eq.(5) is introduced into (6) and (7) is obtained.

$$\dot{x}_N \sin \theta_j - \dot{y}_N \cos \theta_j - h\dot{\theta}_j - 2h \sum_{i=1}^{j-1} \dot{\theta}_i \cos (\theta_i - \theta_j) = 0 \tag{7}$$

Set auxiliary functions are $E_1 = \begin{bmatrix} \sin \theta_1 & -\cos \theta_1 \\ \sin \theta_2 & -\cos \theta_2 \\ \cdots & \cdots \\ \sin \theta_N & -\cos \theta_N \end{bmatrix}$ and

$$E_2 = \begin{bmatrix} h & & & & 0 \\ 2h\cos(\theta_2 - \theta_1) & h & & & \\ 2h\cos(\theta_3 - \theta_1) & 2h\cos(\theta_3 - \theta_2) & h & & \\ \cdots & \cdots & \cdots & \ddots & \\ 2h\cos(\theta_N - \theta_1) & 2h\cos(\theta_N - \theta_2) & 2h\cos(\theta_N - \theta_3) & \cdots & h \end{bmatrix},$$

the velocity of the head joint is $\dot{X}_N = \begin{bmatrix} \dot{x}_N & \dot{y}_N \end{bmatrix}$, the link angles is $\boldsymbol{\theta} = \begin{bmatrix} \theta_1 & \theta_2 & \cdots & \theta_N \end{bmatrix} \in \mathbb{R}^N$, the auxiliary matrix is

$$D = \begin{bmatrix} 1 & -1 & & 0 \\ & \ddots & \ddots & \\ 0 & & 1 & -1 \end{bmatrix} \in \mathbb{R}^{(N-1) \times N}. \text{ Simplified (7) gives (8).}$$

$$E_1 \dot{X}_h^T - E_2 \dot{\boldsymbol{\theta}}^T = 0 \tag{8}$$

Simplification gets $\dot{\boldsymbol{\theta}}^T = E_2^{-1} E_1 \dot{X}_h^T$, and $\varphi_j = \theta_j - \theta_{j+1}$, $\boldsymbol{\varphi} = [\varphi_1, \ldots, \varphi_{N-1}] \in \mathbb{R}^{N-1}$, there are $\boldsymbol{\varphi} = D\boldsymbol{\theta}^T$. So there is (9).

$$\dot{\boldsymbol{\varphi}} = D\dot{\boldsymbol{\theta}}^T = DE_2^{-1} E_1 \dot{X}_h^T \tag{9}$$

The (9) describes the angular velocity $\dot{\boldsymbol{\varphi}}$ of each joint along the axis direction during the motion of a multi-joint snake-like robot. At the same time, the overall angular velocity of the snake-like robot is determined by the angular velocity $\dot{X}_h^T$ of the robot head, the centroid coordinate is $\boldsymbol{p} = \begin{bmatrix} p_x & p_y \end{bmatrix}$, and the angular velocity of each joint is determined by the position of each joint [34]. The relationship between the displacement velocity of each joint $\dot{W}_j$ along the displacement velocity $(\dot{x}_j, \dot{y}_j)$ of the center of mass of the snake-like robot is shown in (10).

$$\begin{cases} \dot{x}_j = \dot{p}_x - \kappa S_\theta \dot{\boldsymbol{\theta}} \\ \dot{y}_j = \dot{p}_y + \kappa C_\theta \dot{\boldsymbol{\theta}} \end{cases}$$

$$\Rightarrow \begin{cases} \dot{x}_j \cos \theta_j = \dot{p}_x \cos \theta_j - \kappa C_\theta S_\theta \dot{\boldsymbol{\theta}} \\ \dot{y}_j \sin \theta_j = \dot{p}_y \sin \theta_j + \kappa C_\theta S_\theta \dot{\boldsymbol{\theta}} \end{cases}$$

$$\Rightarrow \dot{x}_j \cos \theta_j + \dot{y}_j \sin \theta_j = \dot{p}_x \cos \theta_j + \dot{p}_y \sin \theta_j = \dot{W}_j \tag{10}$$

where, the centroid velocity is $\dot{\boldsymbol{p}} = \begin{bmatrix} \dot{p}_x & \dot{p}_y \end{bmatrix}$, the auxiliary function are $S_\theta = diag(\sin \theta_1, \sin \theta_2, \ldots, \sin \theta_N) \in \mathbb{R}^N$ and $C_\theta = diag(\cos \theta_1, \cos \theta_2, \ldots, \cos \theta_N) \in \mathbb{R}^N$, the link angles is $\boldsymbol{\theta} = diag(\theta_1, \theta_2, \ldots, \theta_N) \in \mathbb{R}^N$, the auxiliary matrix is

$$\kappa = \begin{bmatrix} a_1 & \cdots & a_{i-1} & \dfrac{a_i + b_i}{2} & b_{i+1} & \cdots & b_N \end{bmatrix},$$

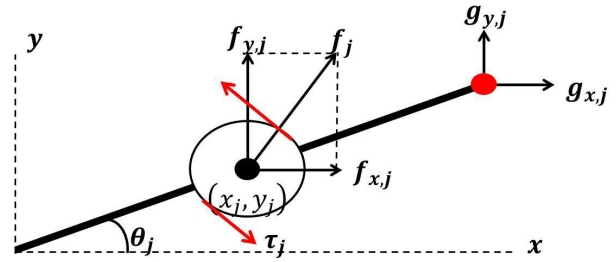$$a_i = \frac{(2i-1)h}{N}, \quad b_i = \frac{(2i-1-2N)h}{N}.$$

FIGURE 2. Force analysis of the *j* th link joint of a multi-joint snake-like robot.

Eq.(10) is decomposed and (11) is obtained.

$$\begin{cases} \dfrac{dx_j}{dW_j} = \cos \theta_j \\ \dfrac{dy_j}{dW_j} = \sin \theta_j \end{cases} \Rightarrow \begin{cases} x_j = \int_0^{W_j} \cos \theta_j dh \\ y_j = \int_0^{W_j} \sin \theta_j dh \end{cases} \tag{11}$$

According to (11), the joint angle curve equation of a multi-joint snake-like robot relative to time variation is obtained as shown in (12).

$$W_j(t) = \int_0^t \sqrt{\dot{x}_j^2 + \dot{y}_j^2} dt \tag{12}$$

B. DYNAMIC MODEL OF A MULTI-JOINT SNAKE-LIKE ROBOT

During the winding motion of the multi-joint snake-like robot, the constraint force of the adjacent link on the $j \in \{1, \ldots, N\}$th joint of the robot is $(g_{x,j}, g_{y,j})$, and the ground friction force on the jth joint of the robot is f_j [16], [32]. On the xOy plane, the driving moment applied by the $j + 1$th link joint on the jth link joint is τ_j, and the driving moment applied by the jth link joint on the $j - 1$th link joint is τ_{j-1}, as shown in Fig. 2.

The force balance of the jth link joint is shown in (13),

$$\begin{cases} m_j \ddot{x}_j = f_{x,j} + g_{x,j} - g_{x,j-1} \\ m_j \ddot{y}_j = f_{y,j} + g_{y,j} - g_{y,j-1} \end{cases} \tag{13}$$

where, $f_{x,j}$ and $f_{y,j}$ are the friction forces along the X-axes and Y-axes of the jth link joint, and m_j is the mass of the jth link joint of the robot [21], [32].

Therefore, the force balance of all links joint is shown in (14).

$$\begin{cases} M\ddot{X}^T = f_{x,j} + D^T g_x \\ M\ddot{Y}^T = f_{y,j} + D^T g_y \end{cases} \tag{14}$$

where, the joint masses is $M = [m_1, m_2, \ldots, m_N] \in \mathbb{R}^N$, the position coordinates are $X = [x_1, x_2, \ldots, x_N] \in \mathbb{R}^N$ and $Y = [y_1, y_2, \ldots, y_N] \in \mathbb{R}^N$, the friction forces are $f_x = [f_{x,1}, f_{x,2}, \ldots, f_{x,N}] \in \mathbb{R}^N$ and $f_y = [f_{y,1}, f_{y,2}, \ldots, f_{y,N}] \in \mathbb{R}^N$, the constraint force of adjacent links are $g_x = [g_{x,1}, g_{x,2}, \ldots, g_{x,N}] \in \mathbb{R}^N$ and

$\mathbf{g}_y = [g_{y,1}, g_{y,2}, \ldots, g_{y,N}] \in \mathbb{R}^N$, the auxiliary matrix is

$$D = \begin{bmatrix} 1 & -1 & & 0 \\ & \ddots & \ddots & \\ 0 & & 1 & -1 \end{bmatrix} \in \mathbb{R}^{(N-1)\times N}.$$

Torque balance of the jth links joint of a multi-joint snake-like robot is shown in (15),

$$J\ddot{\theta}_j = \tau_j - \tau_{j-1} + u_i - u_{i-1} + h\cos\theta_j(g_{y,j} + g_{y,j-1})$$
$$-h\sin\theta_j(g_{x,j} + g_{x,j-1}) \quad (15)$$

where, the friction torque is $\tau = diag(\tau_1, \tau_2, \ldots \tau_N) \in \mathbb{R}^N$, the torque applied by the driving motor is u_i, the inertia moment of the links is $J = diag(J_{s1}, J_{s2}, \ldots, J_{sN}) \in \mathbb{R}^N$ [29]. Therefore, the torque balance of all links of a multi-joint snake-like robot is shown in (16).

$$J\ddot{\theta} = \tau + D^T u_i + hC_\theta A^T g_y - lS_\theta A^T g_x \quad (16)$$

where, auxiliary function are $S_\theta = diag(\sin\theta_1, \sin\theta_2, \ldots, \sin\theta_N) \in \mathbb{R}^N$ and $C_\theta = diag(\cos\theta_1, \cos\theta_2, \ldots, \cos\theta_N) \in \mathbb{R}^N$, the link angles is $\theta = diag(\theta_1, \theta_2, \ldots, \theta_N) \in \mathbb{R}^N$, the velocities is $u_i = diag(u_1, u_2, \ldots, u_N) \in \mathbb{R}^N$, the auxiliary matrix is

$$A = \begin{bmatrix} 1 & 1 & 0 & 0 \\ 0 & \ddots & \ddots & 0 \\ 0 & 0 & 1 & 1 \end{bmatrix} \in \mathbb{R}^{(N-1)\times N}.$$

In order to study the dynamic characteristics of a multi-joint snake-like robot, the constraint conditions (1) between the joints and links of the robot are used to express the constraint conditions of all links of the snake-like robot in matrix form as shown in (17) [21], [32].

$$\begin{cases} DX^T = -hAC_\theta \\ DY^T = -hAS_\theta \end{cases} \quad (17)$$

Eq.(17) is quadratic differentiated and (18) is obtained,

$$\begin{cases} D\ddot{X}^T = hA(C_\theta\dot{\theta}^2 + S_\theta\ddot{\theta}^2) \\ D\ddot{Y}^T = hA(S_\theta\dot{\theta}^2 - C_\theta\ddot{\theta}^2) \end{cases} \quad (18)$$

where, $\dot{\theta}^2 = diag(\dot{\theta}_1^2, \dot{\theta}_2^2, \ldots, \dot{\theta}_N^2) \in \mathbb{R}^N$.

The total mass of the multi-joint snake-like robot is $m = \sum_{i=1}^N m_i$, the centroid coordinate is $p = [p_x \ p_y]$, an auxiliary matrix is $e = [1, \ldots, 1] \in \mathbb{R}^N$, and the centroid position of the multi-joint snake-like robot in the global coordinate system is shown in (19) [29], [32].

$$p^T = \begin{bmatrix} p_x \\ p_y \end{bmatrix} = \begin{bmatrix} \frac{1}{mN}\sum_{i=1}^N m_i x_i \\ \frac{1}{mN}\sum_{i=1}^N m_i y_i \end{bmatrix} = \frac{1}{m}\begin{bmatrix} eMX \\ eMY \end{bmatrix} \quad (19)$$

Add an auxiliary function $L = \left[D, \frac{M^T e}{m}\right] \in \mathbb{R}^n$ or $L^{-1} = \left[M^{-1}D^T\left(DM^{-1}D^T\right), e\right] \in \mathbb{R}^n$. (17) and (19) are combined

to obtain the common attitude model of the center of mass and the link joint of the multi-joint snake-like robot as shown in (20).

$$\begin{cases} LX = [-hA\cos\theta, p_x]^T \\ LY = [-hA\sin\theta, p_y]^T \end{cases} \quad (20)$$

Eq.(21) is obtained by multiplying the left side of (18) by LM^{-1} or $\left[D, \frac{M^T e}{m}\right]M^{-1}$. Where, the acceleration sum of the links joint of the multi-joint snake-like robot is $eD^T = 0$. At the same time, the joint constraints in the centroid coordinates $\ddot{p} = \begin{bmatrix} \ddot{p}_x & \ddot{p}_y \end{bmatrix}$ of the robot are $(g_x, g_y) = 0$.

$$\begin{cases} L\ddot{X} = \begin{bmatrix} D\ddot{X} \\ \ddot{p}_x \end{bmatrix} = \begin{bmatrix} DM^{-1}f_x + DM^{-1}D^T g_x \\ \frac{ef_x}{m} \end{bmatrix} \\ L\ddot{Y} = \begin{bmatrix} D\ddot{Y} \\ \ddot{p}_y \end{bmatrix} = \begin{bmatrix} DM^{-1}f_y + DM^{-1}D^T g_y \\ \frac{ef_y}{m} \end{bmatrix} \end{cases} \quad (21)$$

Eq. (20) and (21) are combined to obtain the joint constraint (22) of the multi-joint snake-like robot (g_x, g_y).

$$\begin{cases} g_x = (DM^{-1}D^T)^{-1}[hA(C_\theta\dot{\theta}^2 + S_\theta\ddot{\theta}) - DM^{-1}f_x] \\ g_y = (DM^{-1}D^T)^{-1}[hA(S_\theta\dot{\theta}^2 - C_\theta\ddot{\theta}) - DM^{-1}f_y] \end{cases} \quad (22)$$

Eq. (22) is introduced into (16) to obtain (23) for the torque balance of the link joint of a multi-joint snake-like robot.

$$[J + hC_\theta A^T(DM^{-1}D^T)^{-1}hAC_\theta + hS_\theta A^T(DM^{-1}D^T)^{-1}hAS_\theta]\ddot{\theta}$$
$$= D^T\tau - hS_\theta A^T(DM^{-1}D^T)^{-1}\left(hAC_\theta\dot{\theta}^2 - DM^{-1}f_x\right)$$
$$+ hC_\theta A^T(DM^{-1}D^T)^{-1}\left(hAS_\theta\dot{\theta}^2 - DM^{-1}f_y\right) \quad (23)$$

According to (21), the centroid acceleration of the link joint is obtained as (24).

$$\begin{cases} \ddot{p}_x = \frac{e^T f_x}{m} \\ \ddot{p}_y = \frac{e^T f_y}{m} \end{cases} \Rightarrow m\ddot{p}^T = \begin{bmatrix} m\ddot{p}_x \\ m\ddot{p}_y \end{bmatrix} = e^T f^T \quad (24)$$

Eq.(24) shows that the centroid acceleration of a multi-joint snake-like robot is only provided by friction. When a state variable $v = \begin{bmatrix} \theta^T, p^T, \dot{\theta}^T, \dot{p}^T \end{bmatrix} \in \mathbb{R}^{2n+4}$ is introduced, the state space form of the robot model is (25). As long as the $\ddot{\theta}$ and $\ddot{p}$ in (25) are solved, the thrust $\Gamma(v, \tau)$ of each joint of the multi-joint snake-like robot can be easily solved.

$$v = \begin{bmatrix} \dot{\theta} \\ \dot{p} \\ \ddot{\theta} \\ \ddot{p} \end{bmatrix}^T = \Gamma(v, \tau) \quad (25)$$

After the multi-joint snake-like robot moves according to certain rules, the friction force and friction moment of each joint of the robot change, and then the acceleration and angular acceleration of the robot change. The change of the acceleration and angular velocity of the robot also
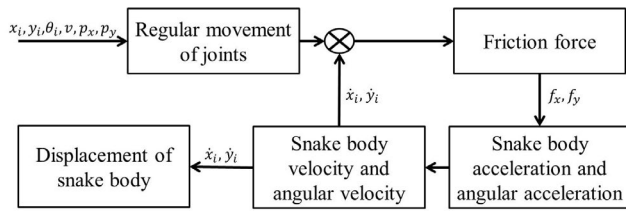
FIGURE 3. Relation among parameters of dynamic model of a snake-like robot.

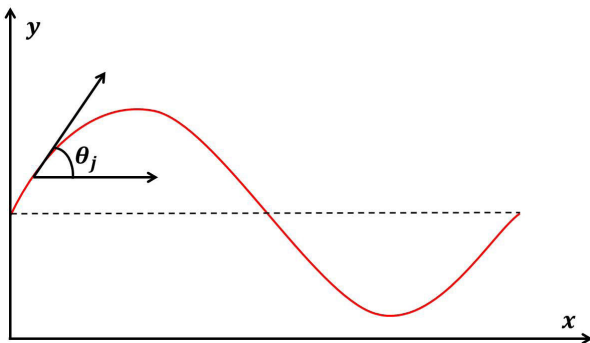**FIGURE 4.** The winding motion of a biological snake.

FIGURE 5. Serpenoid curve.

pull the change of the friction force and friction moment of each joint of the robot. This continuous iteration changes the displacement and motion orientation of the multi-joint snake-like robot, as shown in Fig.3. Friction occurs between the multi-joint snake-like robot and ground. This friction is the key to solving the overall motion law of the robot. It interacts with the motion mode, velocity and angular velocity of each joint of the robot until the robot moves to a stable state.

III. IMPROVEMENT OF SERPENOID CURVE EQUATION

In this section, the locomotion pattern of biological snakes on land and its motion state in the winding motion are observed as shown in Fig.4 [35]. The Serpenoid curve equation (26) proposed by Professor Hirose in Japan is referred [7], as shown in Fig.5.

$$\theta_j(t) = \alpha \sin(\omega t + (j - 1)\delta) \quad j = 1, 2, 3, \ldots, N \quad (26)$$

where, α is the amplitude, ω is the frequency of the swing periodic, and δ is the moving phase between adjacent links. In the calculation, the α, ω and δ are constant, which brings no change in the motion state of the multi-joint snake-like robot. The turning of each link joint of the robot is mechanical and not smooth enough. At the same time, the Serpenoid curve equation lacks an Angle at which to turn, which results in the fact that the Serpenoid curve equation only enables the robot to move forward in the manner of the Serpenoid curve.

According to the kinematics link model of the multi-joint snake-like robot and the curve (12) of joint angle of the robot relative to time variation, this paper presents a motion planning algorithm of the multi-joint snake-like robot with improved Serpenoid curve equation. The algorithm introduces an adjusting factor of joint angle amplitude and an axial bending moment (27) of turning angle adjusting factor at the tail of the robot. When the robot encounters the obstacles, the robot needs to deflect. At this time, the swing phase changes and helps the robot with turning. At the same time, as the joint velocity of the robot changes, the amplitude of the axial bending moment function also changes in response, which ensures the continuity of the joint angle change of the robot. The proposed axial bending moment function not only establishes the relationship between the velocity of each joint and the swing amplitude of the robot, but also enables the robot to overcome obstacles smoothly. The proposed motion planning algorithm adds a feedback with the robot velocity integral to the Serpenoid curve equation. This feedback is an amplitude adjustment factor. When the joint angle of the robot changes, the swing amplitude of the robot also changes, which ensures the continuity of the joint angle. The velocity of the robot varies over a small range. By associating the motion velocity of the robot with the swing amplitude, the amplitude of the robot changes linearly at different velocity, which greatly increases the smoothness of the motion control of the multi-joint snake robot.

$$\theta_j(t) = \alpha \int_0^t \sqrt{\dot{x}_{j-1}^2 + \dot{y}_{j-1}^2} \, dt \, \sin(\omega t + (j - 1)\delta) + \psi$$
$$j = 1, 2, 3, \ldots, N \quad (27)$$

where, α is the swing amplitude of the link joint, $\dot{x}_{j-1}$ and $\dot{y}_{j-1}$ are the velocity of the $j - 1$th joints of the robot, ψ is the turning angle adjustment factor, δ are the angular phase displacement of each link to its adjacent link, ω is the frequency of the swing periodic, t is time variable.

As the proposed motion planning algorithm links the amplitude to the velocity integral of the multi-joint snake-like robot, when the initial velocity of the robot is 0, there is $\theta_j(t) \equiv 0$, and, the robot cannot move at this moment. So we should set an initial velocity for the multi-joint snake, even if it is a small initial velocity. In the moving process of the multi-joint snake-like robot, the position and velocity is constantly updated. Since there is friction during the moving process, the acceleration a of the robot can be calculated according to Newton's Second Law. The acceleration varies with time, position and velocity, and the acceleration directly affects the motion velocity of the robot, which affects the swing amplitude of the robot. When the multi-joint serpentine robot is moving towards a direction, the acceleration increases continuously, which lead to continuous increase of the robot's moving velocity and the robot's swing amplitude. But the swing amplitude cannot increase definitely. When the swing amplitude of the snake reaches extreme value, the joints need to change the directions of swing and rotation positions. At this time, the acceleration changes to $a < 0$
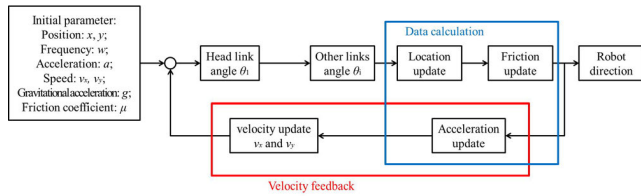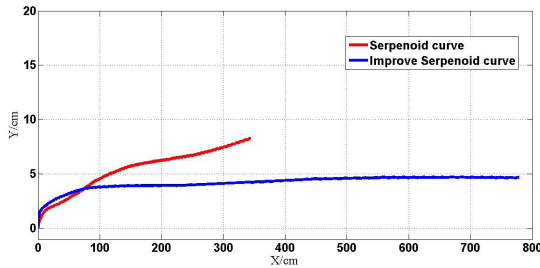
FIGURE 6. Design of motions of the robot.

FIGURE 7. The trajectory of the robot's head.

FIGURE 8. The amplitude adjustment factor change curve of the multi-joint snake-like robot.

FIGURE 9. The acceleration in the X-axis of the multi-joint snake-like robot.

FIGURE 10. The acceleration in the Y-axis of the multi-joint snake-like robot.

FIGURE 11. The rotation angle of the head of the multi-joint snake-like robot.

rapidly, which causes the rapid decrease of the robot's motion velocity and its swing amplitude. As the robot's joints change its swing directions, the acceleration *a* changes from negative to positive and then increases continuously, starting a new cycle of change. During the whole process, even if the angle changes slowly and the linear velocity decreases, as long as the acceleration exists, the linear velocity will not decrease to zero. When the robot moves around a corner, the acceleration will make the linear velocity of the robot increase again. The motion planning and design of the robot are shown in Fig. 6.

In the experiment, the friction coefficient is $\mu = 0.2$, the gravitational acceleration is g $= 9.8$ m/s^2, the swing amplitude of the joint link is $\alpha = \frac{10\pi}{180}$, the angular phase displacement of each link between its adjacent links is $\delta = \frac{\pi}{2}$, the initial velocity is $v_x = v_y = 0.1$ m/s, the calculation time is $t = 25$ *s*, the joint length is L $= 1$ m, and the joint mass is m $= 1$ kg. MATLAB simulation software was used to compare the movement trajectory of the head of the Serpenoid curve equation and the improved Serpenoid curve equation, as shown in Fig. 7. It can be clearly seen from Fig. 7 that the movement trajectory of the head of the multi-joint snake-like robot shows a small displacement phenomenon at the initial moment, which is caused by a small vibration caused by friction during the movement of the robot. Meanwhile, the motion distance of the robot under the action of the improved Serpenoid curve equation motion planning was significantly greater than that under the action of the Serpenoid curve equation motion planning within the same time. This shows that the improved Serpenoid curve equation can provide faster motion velocity for the robot. In terms of the stability of the motion of the multi-joint snake-like robot, the improved Serpenoid curve equation added a joint angle amplitude adjustment factor relative to time and a turning angle adjustment factor at the initial moment, resulting in rapid deflection of the robot and reduced stability.
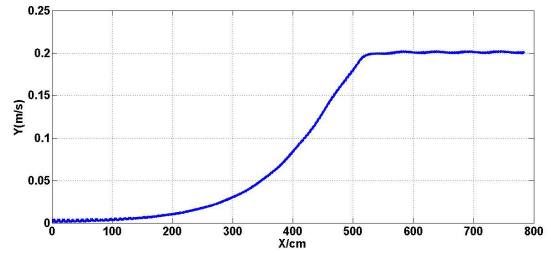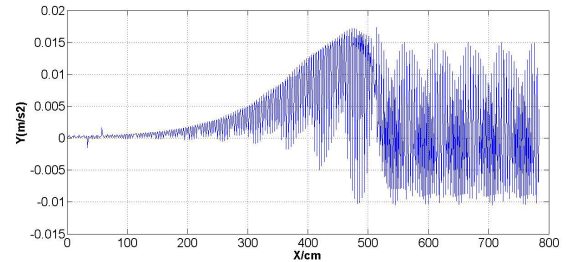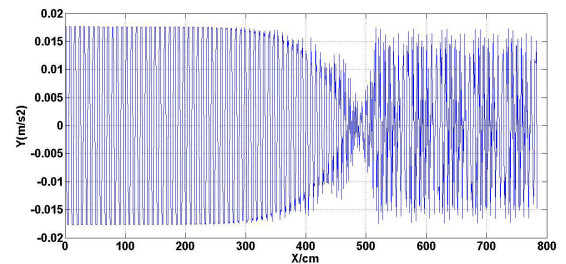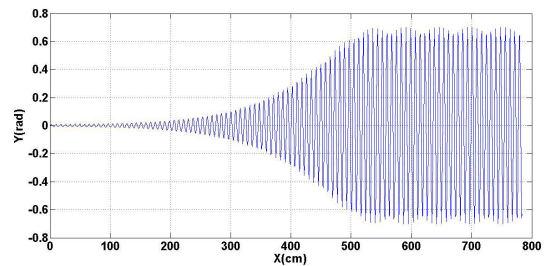
However, after the robot has been in motion for a period of time, the improved Serpenoid curve equation can gradually stabilize the motion trajectory of the robot head, thus the smoothness and stability of the motion control of the multi-joint snake-like robot are greatly increased.

The change curve of the amplitude adjustment factor is shown in Fig.8, the motion acceleration of the multi-joint snake-like robot is shown in Fig.9 and Fig.10, and the rotation
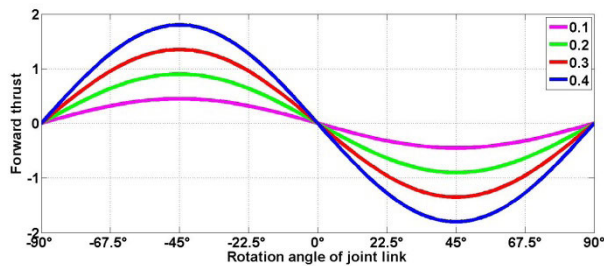
FIGURE 12. The relation between rotation angle of link joints and forward thrust of the robot.

angle of the robot's head is shown in Fig.11. As can be seen from Fig.8 to Fig.11 that when the motion distance of the robot is less than 100cm, the adjustment factor of the amplitude, the motion acceleration in the x direction and the rotation angle of the head change very slowly. At this time, the motion trajectory of the robot head deflected under the action of friction. When the motion distance of the robot is within 100~500cm, the amplitude adjustment factor, the motion acceleration in the X-axis and the rotation angle of the head increase rapidly, while the motion acceleration in the Y-axis decreases. Then the robot enters adjustment phase. At this point, the trajectory of the robot head is slightly adjusted. When the motion distance of the robot is 500cm away, the adjustment factor of joint angle amplitude reaches a stable state. The value of the adjustment factor of joint angle amplitude basically does not change any more. The motion acceleration in the X-axis and Y-axis and the rotation angle of the head show even and stable changes.

According to (25), the relationship between the rotation angle $\boldsymbol{\theta}(t)$ of the link joint and the forward thrust $\boldsymbol{\Gamma}(v, \tau)$ is obtained, as shown in Fig.12. As can be seen from Fig.12 that $\boldsymbol{\Gamma}(v, \tau)$ takes an extreme value at $\theta_j(t) = \pm\frac{\pi}{4}$. This shows that when the vertical velocity $\dot{y}_j$ and forward direction of the link of the multi-joint snake-like robot is $\pm\frac{\pi}{4}$, the thrust of the tail joint of the robot to the head joint is the largest. It can be seen from (27) that the forward thrust amplitude $\left|\Gamma_j\right|$ of the jth link of the robot can be increased by increasing the vertical velocity amplitude $\left|\dot{y}_j\right|$ of the robot when the rotation angle of the link joint is $\left|\theta_j(t)\right| < \frac{\pi}{4}$.

The axial bending moment (27) with the amplitude adjustment factor and turning angle adjustment factor is differentiated, and the angular velocity (28) of each link joint is obtained.

$$\dot{\theta}_j(t) = \alpha \left(\dot{x}_{j-1}^2 + \dot{y}_{j-1}^2\right) \sin(\omega t + (j-1)\delta)$$
$$+ \alpha\omega \int_0^t \sqrt{\dot{x}_{j-1}^2 + \dot{y}_{j-1}^2} \, dt \cos(\omega t + (j-1)\delta)$$
$$j = 1, 2, 3, \ldots, N \quad (28)$$

The velocity of each link of the multi-joint snake-like robot is given by (5). The initial velocity is $\dot{x}_h = 0$, $\dot{y}_h = 0$. In the calculation process, the number of joints of the multi-joint

snake robot is $N = 6$. Substitute (28) into (5) to get (29).

$$\dot{y}_j = \begin{cases} \alpha h \sin \omega t \cos\left[\alpha \int_0^t \sqrt{\dot{x}_0^2 + \dot{y}_0^2} \, dt \sin \omega t + \psi\right] & j = 1 \\ 2\alpha h \sum_{j=2}^{N-1} \sin\left(\omega t + (j-2)\delta + \beta_{j-1}\right) \\ + \alpha h \sin\left(\omega t + (j-1)\delta + \beta_{j-1}\right) & j > 1 \\ \cos\left[\alpha \int_0^t \sqrt{\dot{x}_{j-1}^2 + \dot{y}_{j-1}^2} \, dt \sin(\omega t + (j-1)\delta) + \psi\right] \end{cases}$$
$$(29)$$

where,

$$\tan \beta_j = \frac{\omega \int_0^t \sqrt{\dot{x}_{j-1}^2 + \dot{y}_{j-1}^2} \, dt}{\dot{x}_{j-1}^2 + \dot{y}_{j-1}^2}, \quad j = 1, 2, 3, \ldots, N \quad (30)$$

By the increase of velocity amplitude $\left|\dot{y}_j\right|$ of the multi-joint snake robot, the forward thrust amplitude generated by the jth of the robot can be increased. It can be seen from (29) that the swing amplitude α, the frequency swing period ω, the joint length h and the motion velocity in XY-axis of the robot directly affect the motion velocity amplitude of the robot's link $\left|\dot{y}_j\right|$. As the swing amplitude α, the frequency swing period ω, the joint length h are fixed, $\left|\dot{y}_j\right|$ changes periodically with the change of the velocity of the robot. In summary, the axial bending moment functions with joint angle amplitude adjustment factor and turning angle adjustment factor adjusts the amplitude indirectly, so that the new swing amplitude of robot change periodically. Thus the path divergence caused by large swing amplitude can be avoided.

During the movement of the robot, the position and velocity of the robot is continuously transferred to the main control module. Through analysis and calculation, the main control module sends the command to the rotating motor of the joint. The rotating motor controls the forward motion of the robot by adjusting the rotation angle and velocity, as shown in Fig.13. As can be seen from Fig.13 that the designed closed-loop system adopts three sets of closed-loop feedback loops. The closed-loop system can not only provide simple, efficient and reliable joint angle and feedback velocity for the multi-joint snake robot, but also realize the overload protection function of the circuit.

IV. SIMULATION

In order to prove the effectiveness of the motion planning algorithm for the multi-joint snake-like robot based on the improved Serpenoid curve equation, this section uses the semi-physical simulation form of robot to verify the algorithm. According to the structure characteristics and motion mechanism of the multi-joint snake-like robot, the real structure model of the robot is established. SimWise4D simulation software was used to simulate the dynamics of the multi-joint snake robot. The relative joint angle input curve, snake tail displacement curve, snake tail velocity curve, driven wheel rotation curve, contact force of driven wheel and friction force of driven wheel are analyzed based on improved Serpenoid curve equation motion planning algorithm. The effects of
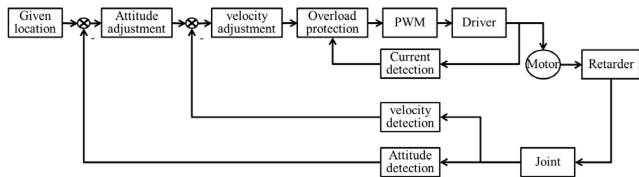
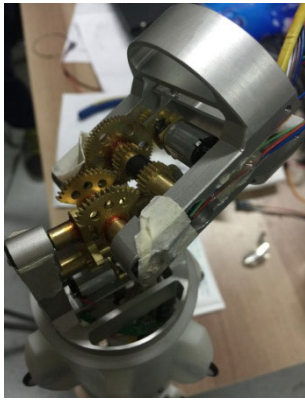**FIGURE 13.** Closed-loop control system.

FIGURE 14. Connection module of the cross universal joint.

FIGURE 15. Joint cabin structure of the multi-joint snake-like robot.
(a) Torso part, (b) Head part.

FIGURE 16. Complete model of the multi-joint snake-like robot.

the swing amplitude α, frequency of the swing periodic ω and the moving phase δ between adjacent links on the forward velocity of the multi-joint snake-like robot is analyzed. The effectiveness of the algorithm is verified by simulation experiments.

A. PHYSICAL MODELING OF THE MULTI-JOINT SNAKE ROBOT

When using virtual prototype software and control system software to simulate multi-joint snake-like robot jointly, the structure of the robot should be designed according to the structural characteristics and motion mechanism of the multi-joint snake-like robot.

By observing the movement mechanism of biological snakes and referring to the snake-like robot ACM-R5 designed by Professor Hirose of Tokyo institute of technology, a kind of snake-like robot with multiple joints composed of the same joint is designed. The robot's joints are connected by a "cross" universal joint. The universal joint is made of metal and has a simple structure, as shown in Fig. 14. Each "cross" universal joint is composed of two independent gears with orthogonal axes. This structure enables each joint of the multi-joint snake-like robot to have two degrees of freedom. It can make the robot simulate the flexible body of the biological snake and realize various forms of motion. A multi-joint snake-like robot motion device with multiple degrees of freedom and redundancy is composed of several universal joints. Each universal joint gear is equipped with a brush DC motor. Each motor controls the rotation velocity and direction of the universal joint with one degree of freedom. As long as the rotation velocity and timing of each brush DC motor are well controlled, various forms of work of the multi-joint snake-like robot can be realized.
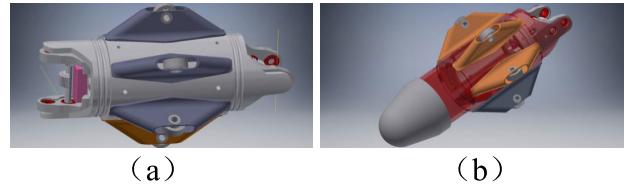
The joint part of the multi-joint snake-like robot adopts a cabin structure, as shown in Fig.15. The "fins" are set in six positions around the cabin, and the driven wheels are set on each "fin" to assist the motion of the robot. The driven wheel itself does not move. The driven wheel only assists the snake body to slide during the torsion of the universal joint of the robot, thus realizing the robot's motion mode based on the improved Serpenoid curve equation. Each cabin structure of the multi-joint snake-like robot is connected with a "cross" universal joint, and thus a complete model of the multi-joint snake-like robot is established, as shown in Fig.16.

B. DYNAMICS SIMULATION OF THE MULTI-JOINT SNAKE-LIKE ROBOT

After establishing the complete model of the multi-joint snake-like robots, the dynamic simulation of the robot is carried out by using SimWise4D multi-entity dynamic simulation software. The relative joint Angle input curve, snake tail displacement curve, snake tail velocity curve, driven wheel rotation curve, driven wheel contact force and driven wheel friction change curve are analyzed during the robot motion. The effects of the swing amplitude of the improved Serpenoid curve equation, the frequency of the swing periodic and the moving phase between adjacent links on the forward velocity of the multi-joint snake-like robot are compared, and the effectiveness of the algorithm is verified.

In the simulation process, the initial environment is set as follows: the friction coefficient is 0.5, the joints are set as motor drive constraints, and the motion process of the multi-joint snake-like robot is shown in Fig.17. The robot maintains a meandering attitude and moves forward under the constraints of the improved Serpenoid curve equation motion planning algorithm. During the movement, the input curve of the relative joints angle of the head joint of the multi-joint snake-like robot is shown in Fig.18. From Fig.18, we can see that the trajectory of the head of the robot is
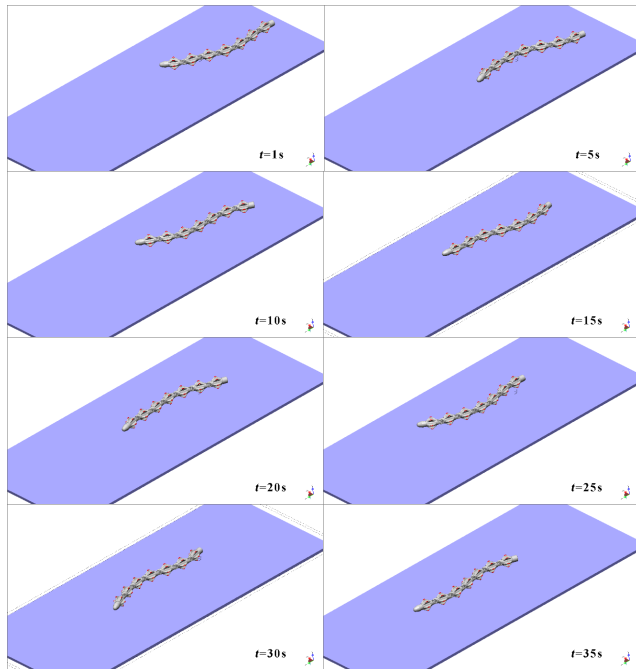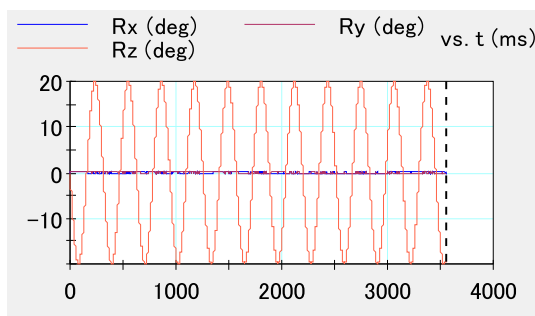
FIGURE 17. Motion process of the robot.

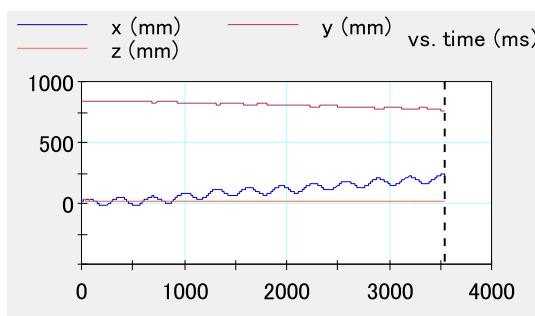FIGURE 18. Head joint angle motion curve of the robot.

FIGURE 19. Displacement curve of the tail of the robot.

FIGURE 20. Velocity curve of the tail of the robot.
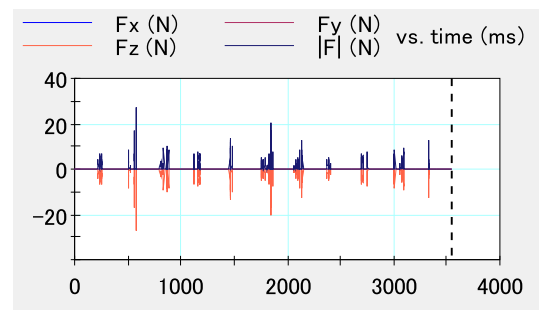
FIGURE 21. Contact force of driven wheel of the robot.

an improved Serpenoid curve equation similar to sine function. This is a smooth trajectory. The displacement curve of the snake tail of a multi-joint snake-like robot is shown in Fig.19. From Fig.19, it can be seen that under the action of friction, the tail trajectory of multi-joint snake-like robot has a small displacement compared with the head trajectory, but the overall motion pattern still follows the improved Serpenoid curve equation. The velocity curve of the snake tail
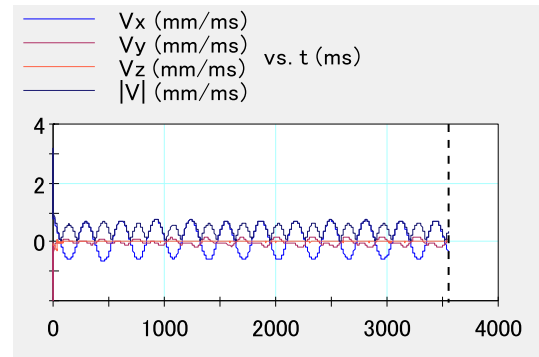
of the multi-joint snake-like robot is shown in Fig.20. As can be seen from Fig.20, the motion velocity of the multi-joint snake-like robot presents a uniform sinusoidal function. This is because the forward velocity of the robot changes with the swing of the tail during its moving process. The swing of the tail presents a sinusoidal waveform and the forward velocity also presents a sinusoidal waveform. The contact force on the tail driven wheel of the multi-joint snake-like robot is shown in Fig.21. As can be seen from Fig. 21, the contact force between the driven wheel and the ground at the tail of the multi-joint snake-like robot changes with the swing amplitude of the driven joint. The greater the swing amplitude of the driven joint, the greater the contact force on the ground to the driven wheel. When the driven joint is restored to equilibrium, the contact force between the driven wheel and the ground is restored to zero. The friction force on the tail driven wheel of the multi-joint snake-like robot is shown in Fig.22. As can be seen from Fig.22, the magnitude of the friction force on the driven wheel is closely related to the ground contact force on the driven wheel. The greater the ground contact force on the driven wheel, the greater the ground friction force on the driven wheel. The smaller the ground contact force on the driven wheel, the smaller the ground friction force on the driven wheel. However, the ground contact force of the driven wheel is positive and negative, and the friction force of the driven wheel is only in the positive direction.

The influence of parameters α, ω and δ in the improved Serpenoid curve equation motion planning (27) on the forward velocity of the multi-joint snake-like robot is shown in Figs.23, 24 and 25. Fig.23 shows that the swing amplitude
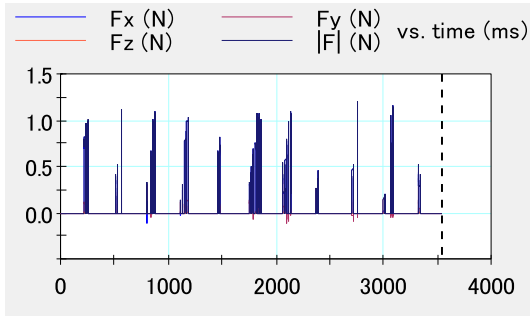
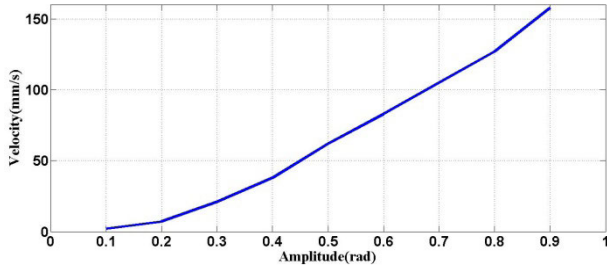**FIGURE 22.** Friction force of driven wheel of the robot.

FIGURE 23. The relation between the forward velocity and the amplitude α of the robot.
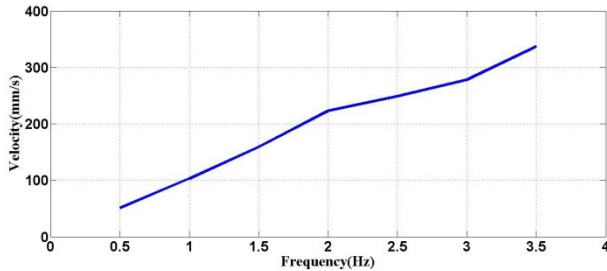

FIGURE 24. The relation between the forward velocity and the frequency of the swing periodic angle ω of the robot.
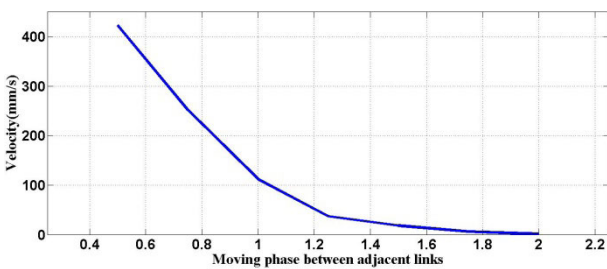

FIGURE 25. The relation between the forward velocity and the moving phase between adjacent links δ of the robot.

of the multi-joint snake-like robot is positively correlated with the forward velocity of the robot. The larger the swing amplitude of the robot, the faster the forward velocity of the robot. However, the swing amplitude of the robot is limited by the maximum rotation angle of the joint and can only move in a certain range. Fig.24 shows that the frequency of the swing periodic of the multi-joint snake-like robot is positively correlated with the forward velocity of the robot. The higher the frequency of the robot, the faster the forward velocity of the robot. However, the frequency of the robot is limited
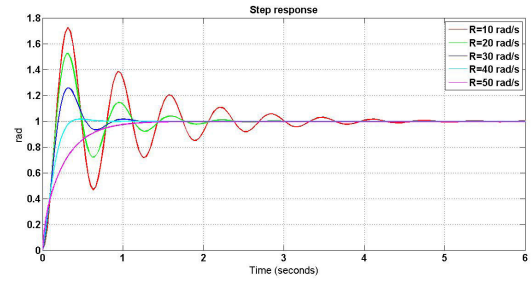

FIGURE 26. The step response of the electric steering gear at different rotational velocities.

by the driving ability of the joint-driven actuator. When the frequency is $\omega > 2$, the forward velocity of the robot increases and the frequency of the swing periodic decreases. Fig.25 shows that the moving phase between adjacent links of the multi-joint snake-like robot is negatively related to the forward velocity of the robot. The larger the moving phase between adjacent links of the robot, the slower the forward velocity of the robot. However, the small moving phase between the adjacent links of the robot will affect the direction of the robot, resulting in the robot can not form a complete Serpenoid curve, affecting the efficiency of the robot.

V. EXPERIMENT

During the movement of the multi-joint snake-like robot, the rotation angles of each joint are controlled by the electric steering gear. Therefore, the dynamic analysis of the electric steering gear at the joints of the robot should be carried out, so as to reduce the required adjustment time T_s when the system reaches overshoot σ_p and make the system enter a stable state as soon as possible. A step signal from 0 to 1 is input at 0s, and the electric steering gear system will follow the reference input at different rotational velocity R. When the rotation velocity is $10 rad/s$, the motion stability response velocity of the multi-joint snake robot is slow. At the same time, it can be found that under the condition of low rotational velocity, the overshoot of the system increases. With the increase of rotational velocity, the overshoot decreases gradually and the adjustment time is shortened. However, the kinematics stability of the multi-joint snake-like robot is lower when the rotational velocity of the electric steering gear is $50 rad/s$ than that when the rotational velocity is $40 rad/s$. In other words, the optimal rotational velocity of the electric steering gear is about $40 rad/s$. The kinematics stability response of the multi-joint snake-like robot is not linearly correlated with the rotational velocity, as shown in Fig. 26. The performance indicators of the step response of the electric steering gear at different rotational velocities are shown in Table 1.

Obviously, when the rotational velocity of the electric steering gear is $40 rad/s$, the motion stability of the robot reaches the optimal response state. When the rotational velocity of the electric steering gear increases to $50 rad/s$, there is no symmetry between the rotational velocity and voltage

TABLE 1. Performance indexes of the electric steering gear at different rotational velocities.

R (rad/s)	10	20	30	40	50
$\sigma_p\,(\%)$	32.7365	15.5421	6.3847	4.9630	13.5041
$T_s\,(s)$	3.8231	2.3696	0.9362	0.5493	1.2565

of the electric steering gear, and the stability of the electric steering gear decreases significantly.

In order to verify the effectiveness of the proposed motion planning algorithm based on improved Serpenoid curve equation, the processing design and physical experiments of the multi-joint snake-like robot prototype are carried out in this section. The multi-joint snake-like robot adopts modular structure. Each module mainly includes wireless transceiver module, reconnaissance and search module, ranging module, main control module, joint module, environmental monitoring module and power module. The control system of the multi-joint snake-like robot uses bus to realize the communication between modules. The multi-joint snake-like robot is powered by lithium batteries, and motion instructions are sent by an infinite Bluetooth module. The battery power meets the needs of the robot for more than 20 minutes of movement time, and the unlimited Bluetooth module meets the needs of the robot for more than 10 meters of communication distance. In order to facilitate the calculation, the joint length of the multi-joint snake-like robot is $h = 211$ *mm*, the joint radius is $r = 65$ *mm*, and the number of joints is $N = 6$. Six groups of driven wheels are distributed evenly in each joint. The friction coefficient of driven wheels is 0.2, and the maximum rotation angle between joints is $\theta = \pm 40°$. Where, a joint is the sum of a cabin and a "cross" universal joint of the robot. The battery capacity is 1500 mAh, the discharge rate of the battery is $3 - 5$ C, the initial phase of the movement between the adjacent links of the robot is $\delta = 0$, the joint mass of the robot is $m = 200$ g, the initial frequency of the swing periodic angle is $\omega = 3$, the gravity acceleration is $g = 9.8\mathrm{N}/\mathrm{kg}$, and the initial swing amplitude of the robot is $\alpha = 0.7$.

The multi-joint snake-like robot was placed on the floor of the corridor to observe the motion of the robot, as shown in Fig.27. From Fig.27, the forward distance of the robot can be judged by observing the relative position between the ground and the multi-joint snake-like robot. The robot can move forward through the improved Serpenoid curve equation. In order to analyze the influence of the swing amplitude and frequency of swing period on the forward velocity of the multi-joint snake-like robot, the experiment adjusts the parameters so that the robot can start from the same place and record the time needed to reach the same target position (68cm). The influence of the swing amplitude on the forward velocity of the multi-joint snake-like robot is analyzed, as shown in Fig.28 and Fig.29. With other parameters unchanged, the swing amplitude α increases, the running time of the robot decreases, the motion velocity increases, and the control efficiency improves, which is consistent with the

FIGURE 27. The multi-joint snake-like robot moving on the floor of corridor.
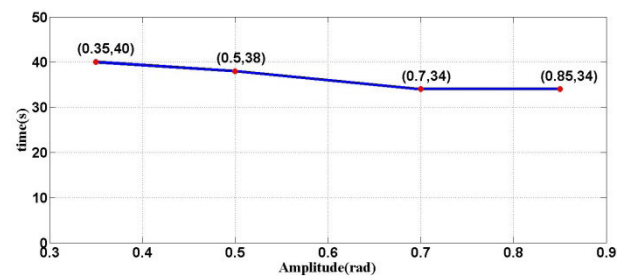
FIGURE 28. Effect of the swing amplitude α on motion time.
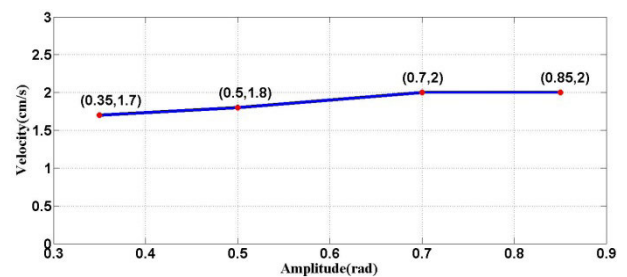
FIGURE 29. Effect of the swing amplitude α on motion velocity.

simulation results of SimWise4D. The influence of the frequency of swing period on the control efficiency of the multi-joint snake-like robot is analyzed, as shown in Fig.30 and Fig.31. When other parameters remain unchanged, the joint angular velocity ω increases, which leads to the acceleration of the frequency of swing period and the increase of the forward velocity of the robot, which is consistent with the simulation results of the dynamic simulation software SimWise4D. At $\omega = 8$, the forward velocity of the multi-joint snake-like robot decreases. This is because the rotation velocity of the robot joints is less than the instruction velocity received, which leads to the next action before the robot joints are rotated in place. Therefore, the parameters need to be adjusted reasonably according to the actual situation.

The motion planning algorithm of the multi-joint snake-like robot with improved Serpenoid curve equation is
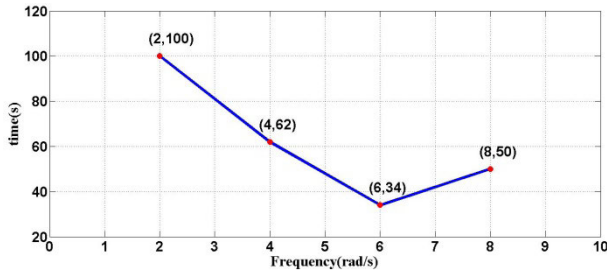
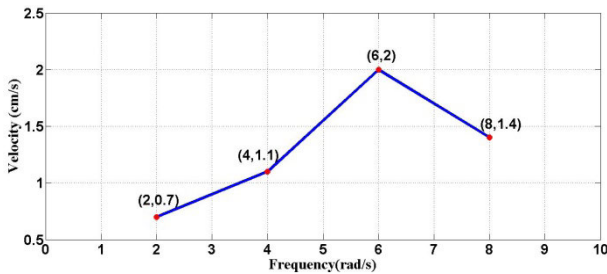**FIGURE 30.** Effect of the frequency of swing period ω on motion time.

FIGURE 31. Effect of the frequency of swing period ω on motion velocity.
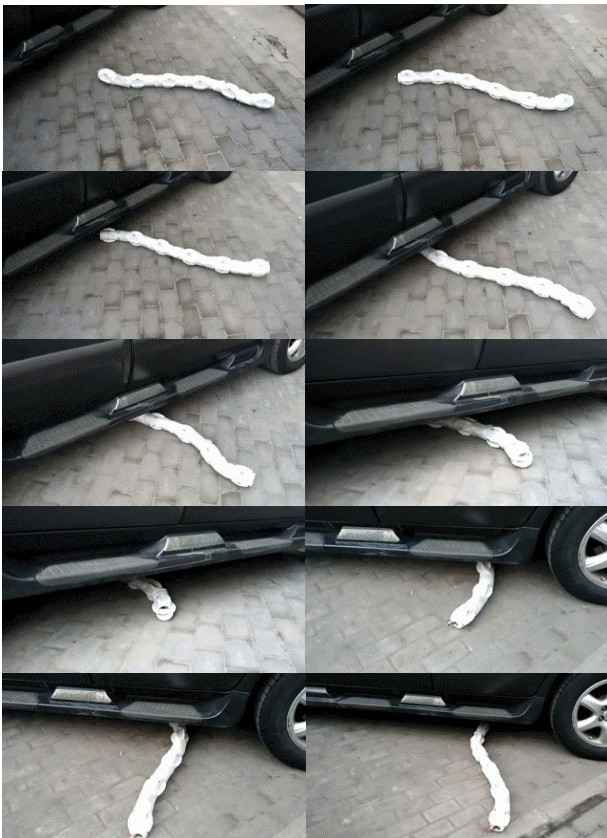

FIGURE 32. The multi-joint snake-like robot traverses the underside of the car.

FIGURE 33. The multi-joint snake-like robot crossing the deceleration belt.

to the other, as shown in figure 32. The motion velocity of the multi-joint snake-like robot is greatly improved, because the friction of the driven wheel is relatively large on the brick road. The tail joint of the robot can provide sufficient forward power for the head joint, so the moving velocity of the robot is improved.

The obstacle jumping experiment of the multi-joint snake-like robot on asphalt pavement is carried out, as shown in Fig. 33. The multi-joint snake-like robot can cross the deceleration belt with a slope of 7° and a height of 50 mm. The robot mainly relies on its rear joints to generate power for moving forward when it crosses obstacles. Because the number of joints of the multi-joint snake robot is small, the robot moves slowly. This requires that the electric steering gear of the multi-joint snake robot at the joint should have enough torque, the electric steering gear fixation should be more reliable, and the gear at the joint should be more consistent. Despite of this, the multi-joint snake-like robot will ultimately cross the deceleration belt, which verifies

validated for the motion characteristics of the robot on brick pavement. Brick pavement has a high roughness, which leads to a great increase in the friction of the robots. In the experiment, the multi-joint snake-like robot is placed beside the car, and the robot crossed the bottom of the car from one side

the effectiveness of the motion planning algorithm based on improved Serpenoid curve equation.

The experimental results show that the proposed multi-joint snake-like robot motion planning algorithm based on improved Serpenoid curve equation can enable the robot to move forward and jump over obstacles on different roads. With the same parameters, the forward velocity of the multi-joint snake-like robot is closely related to the friction coefficient of the ground and the condition of the ground. Generally, the rougher the ground is, the greater the friction coefficient is, and the faster the robot moves forward. The proposed algorithm is accurate and feasible, and experiments verified the effectiveness of the improved Serpenoid curve equation motion planning algorithm.

VI. CONCLUSION

In this paper, a motion planning algorithm of a multi-joint snake-like robot based on improved Serpenoid curve equation is proposed, which realizes the snake-like robot's winding and sideslip motion in the plane. Firstly, the kinematics model of a multi-joint snake-like robot is established, and the structure and joint characteristics of the robot are analyzed. The joint angle curve equation of the robot relative to time is obtained. Through the dynamic modeling of a multi-joint snake-like robot, the dynamic characteristics between the motion velocity and friction of the link joint are analyzed, and the thrust expressions of the joints of a multi-joint snake-like robot are obtained. Next, according to the joint angle curve equation and Serpenoid curve equation of the multi-joint snake-like robot relative to time variation, the axial bending moment function of the robot with the amplitude adjustment factor and a turning angle adjustment factor is deduced. According to the thrust expression of the multi-joint snake-like robot, the relationship between the forward thrust of the robot and the improved Serpenoid curve equation is analyzed. A simple, efficient and reliable closed-loop control system for multi-joint snake-like robot is designed. Then, the link joint model of the multi-joint snake-like robot is simulated by using MATLAB. The motion mode and trajectory of the robot are analyzed. The simulation validity of the algorithm is verified. SimWise4D multi-entity dynamic simulation software is used for semi-physical modeling and simulation of the multi-joint snake robot. The relative joint angle input curve, snake tail displacement curve, snake tail velocity curve, driven wheel rotation curve, contact force of driven wheel and friction force of driven wheel are analyzed. The effects of the swing amplitude, the frequency of the swing period and the moving phase between adjacent links of the improved Serpenoid curve equation on the forward velocity of the multi-joint snake-like robot are compared, and the effectiveness of the algorithm is verified. Finally, the multi-joint snake-like robot is placed on different roads for experiments, and the influences of the swing amplitude of the robot on the motion velocity and time of the robot are analyzed. The effectiveness of the motion planning algorithm

of the multi-joint snake-like robot based on the improved Serpenoid curve equation is verified.

REFERENCES

[1] N. Zhong, X. Li, Z. Yan, and Z. Zhang, "A neural control architecture for joint-drift-free and fault-tolerant redundant robot manipulators," *IEEE Access*, vol. 6, pp. 66178–66187, 2018.
[2] X. S. Papageorgiou, C. S. Tzafestas, P. Maragos, G. Pavlakos, G. Chalvatzaki, G. Moustris, I. Kokkinos, A. Peer, B. Stanczyk, E.-S. Fotinea, and E. Efthimiou, "Advances in intelligent mobility assistance robot integrating multimodal sensory processing," in *Proc. Int. Conf. Universal Access Hum.-Comput. Interact.*, 2014, pp. 692–703.
[3] P. Shi, Q. Shao, and D. Liang, "Design and improved serpentine curve locomotion control of a planar modular snake robot," in *Proc. IEEE Int. Conf. Inf. Autom. (ICIA)*, Aug. 2016, pp. 1398–1402.
[4] L. Liu, S. Liu, Y. Wu, Y. Yang, Y. Gao, and F.-C. Wang, "Flexibility optimized control for robot efficient moving in corridors based on viability theory," *IEEE Access*, vol. 7, pp. 103583–103594, 2019.
[5] Y. S. Krieger, D. B. Roppenecker, I. Kuru, and T. C. Lueth, "Multi-arm snake-like robot," in *Proc. IEEE Int. Conf. Robot. Autom. (ICRA)*, May 2017, pp. 2490–2495.
[6] J. Gray, "The mechanism of locomotion in snakes," *J. Exp. Biol.*, vol. 23, pp. 101–120, Dec. 1946
[7] H. Yamada and S. Hirose, "Approximations to continuous curves of active cord mechanism made of arc-shaped joints or double joints," in *Proc. IEEE Int. Conf. Robot. Autom.*, May 2010, pp. 703–708.
[8] D. Rincon and J. Sotelo, "Dynamic and experimental analysis for inch-wormlike biomimetic robots ver-vite," *IEEE Robot. Autom. Mag.*, vol. 10, no. 4, pp. 53–57, Dec. 2003.
[9] K. Mcisaac and J. Ostrowski, "Motion planning for anguilliform locomotion," *IEEE Trans. Robot. Autom.*, vol. 19, no. 4, pp. 637–652, Aug. 2003.
[10] P. Liljeback, K. Pettersen, and O. Stavdahl, "Modelling and control of obstacle-aided snake robot locomotion based on jam resolution," in *Proc. IEEE Int. Conf. Robot. Autom.*, May 2009, pp. 3807–3814.
[11] Y.-H. Lv, L. Li, M.-H. Wang, and X. Guo, "Simulation study on serpentine locomotion of underwater snake-like robot," *Int. J. Control Autom.*, vol. 8, no. 1, pp. 373–384, Jan. 2015.
[12] S. Ma, N. Tadokoro, B. Li, and K. Inoue, "Analysis of creeping locomotion of a snake robot on a slope," in *Proc. IEEE Int. Conf. Robot. Autom.*, vol. 2, Mar. 2004, pp. 2073–2078.
[13] S. Ma, "Analysis of snake movement forms for realization of snake-like robots," in *Proc. IEEE Int. Conf. Robot. Autom.*, vol. 4, Jan. 2003, pp. 3007–3013.
[14] M. Sato, M. Fukaya, and T. Iwasaki, "Serpentine locomotion with robotic snakes," *IEEE Control Syst.*, vol. 22, no. 1, pp. 64–81, Feb. 2002.
[15] M. Tanaka, K. Tanaka, and F. Matsuno, "Approximate path-tracking control of snake robot joints with switching constraints," *IEEE/ASME Trans. Mechatronics*, vol. 20, no. 4, pp. 1633–1641, Aug. 2015.
[16] R. Ariizumi and F. Matsuno, "Dynamic analysis of three snake robot gaits," *IEEE Trans. Robot.*, vol. 33, no. 5, pp. 1075–1087, Oct. 2017.
[17] F. Boyer, M. Porez, and W. Khalil, "Macro-continuous computed torque algorithm for a three-dimensional eel-like robot," *IEEE Trans. Robot.*, vol. 22, no. 4, pp. 763–775, Aug. 2006.
[18] F. Matsuno and H. Sato, "Trajectory tracking control of snake robots based on dynamic model," in *Proc. IEEE Int. Conf. Robot. Autom.*, Apr. 2005, pp. 3029–3034.
[19] R. L. Hatton and H. Choset, "Sidewinding on slopes," in *Proc. IEEE Int. Conf. Robot. Autom.*, May 2010, pp. 691–696.
[20] S. Takaoka, H. Yamada, and S. Hirose, "Snake-like active wheel robot ACM-R4.1 with joint torque sensor and limiter," in *Proc. Int. Conf. Intell. Robots Syst.*, Sep. 2011, pp. 1081–1086.
[21] A. Mohammadi, E. Rezapour, M. Maggiore, and K. Y. Pettersen, "Maneuvering control of planar snake robots using virtual holonomic constraints," *IEEE Trans. Control Syst. Technol.*, vol. 24, no. 3, pp. 884–899, May 2016.
[22] E. Rezapour, K. Y. Pettersen, P. Liljeback, and J. T. Gravdahl, "Path following control of planar snake robots using virtual holonomic constraints," in *Proc. IEEE Int. Conf. Robot. Biomimetics (ROBIO)*, Dec. 2013, pp. 530–537.
[23] E. Rezapour, A. Hofmann, and K. Y. Pettersen, "Maneuvering control of planar snake robots based on a simplified model," in *Proc. IEEE Int. Conf. Robot. Biomimetics (ROBIO)*, Dec. 2014, pp. 548–555.

[24] Y. Hu, L. Zhang, W. Li, and G.-Z. Yang, "Design and fabrication of a 3-D printed metallic flexible joint for snake-like surgical robot," *IEEE Robot. Autom. Lett.*, vol. 4, no. 2, pp. 1557–1563, Apr. 2019.

[25] J. Huang, H. Wang, L. Cui, S. Tian, and F. Zhang, "Modeling of notched variable stiffness continuum flexible snake-like robot," in *Proc. Int. Autom. Control Conf. (CACS)*, Nov. 2018.

[26] D. Li, Z. Pan, H. Deng, and T. Peng, "Trajectory tracking control law of multi-joint snake-like robot based on improved snake-like curve in flow field," *Int. J. Adv. Robotic Syst.*, vol. 16, no. 2, Mar. 2019, Art. no. 172988141984466.

[27] Y. Liu, Q. Yan, Q. Zhang, W. Guo, Odbal, B. Wu, and Z. Wang, "Control system design and implementation of flexible multi-joint snake-like robot for inspecting vessel," in *Proc. Int. Conf. Intell. Auton. Syst.*, vol. 531, 2017, pp. 1037–1047.

[28] L. Wang, Q. Guo, Z. Wei, and Y. Liu, "Spatial conflict resolution in a multi-agent process by the use of a snake model," *IEEE Access*, vol. 5, pp. 24249–24261, 2017.

[29] E. Rezapour, "Model-based locomotion control of underactuated snake robobots," Ph.D. dissertation, NTNU, Trondheim, Norway, 2015.

[30] H. Kalani, A. Akbarzadeh, and H. Bahrami, "Application of statistical techniques in modeling and optimization of a snake robot," *Robotica*, vol. 31, no. 4, pp. 623–641, Jul. 2013.

[31] W. Shen, Z. Pan, M. Li, and H. Peng, "A lateral control method for wheel-footed robot based on sliding mode control and steering prediction," *IEEE Access*, vol. 6, pp. 58086–58095, 2018.

[32] W. Ouyang, W. Liang, C. Li, H. Zheng, Q. Ren, and P. Li, "Steering motion control of a snake robot via a biomimetic approach," *Frontiers Inf. Technol. Electron. Eng*, vol. 20, no. 1, pp. 32–44, Jan. 2019.

[33] Ş. Yildirim and K. A. Ben-Aziz, "Design and proposed model reference trajectory control of a snake like robot," in *Proc. Int. Workshop Comput. Kinematics*, vol. 52, 2018, pp. 191–199.

[34] L. Tang, J. Huang, L.-M. Zhu, X. Zhu, and G. Gu, "Path tracking of a cable-driven snake robot with a two-level motion planning method," *IEEE/ASME Trans. Mechatronics*, vol. 24, no. 3, pp. 935–946, Jun. 2019.

[35] D. L. Hu, J. Nirody, T. Scott, and M. J. Shelley, "The mechanics of slithering locomotion," *Proc. Nat. Acad. Sci. USA*, vol. 106, no. 25, pp. 10081–10085, Jun. 2009.
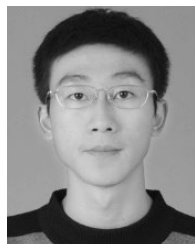
CHAO WANG was born in Chongqing, in 1988. He received the B.E. degree in mechanical and electrical engineering from the Beijing Institute of Technology, in June 2011, and the Ph.D. degree in armament science and technology from the Beijing Institute of Technology, in June 2017. He studied the actuator servo control systems, the snake-like robot, ad hoc robot and micro high speed data recorder in the National Key Laboratory of Electro-Mechanical System and Control, School of Mechatronics Engineering. He is currently an Engineer in China North Industries Corp.

He participated in several scientific research projects, published some conference and journal articles, applied and authorized six national defense patents, two national inventions, one software copyright, and one professional book. He had been awarded first class scholarship and Tang Nanjun Scholarship of the Beijing Institute of Technology. His research interests are robotics, control, electronic design, and weapon system design.

HONGBIN DENG was born in Sichuan, in 1975. He is currently pursuing the Ph.D. degree with the Beijing Institute of Technology. He is also an Associate Professor with the Beijing Institute of Technology.

He has been engaged in robot design, engineering mechanics, pattern recognition, mathematical modeling, simulation, optimization, system integration and other fields for a long time. The researches focus on system design, control algorithm design and optimization, mechanism dynamic simulation, and so on.

DONGFANG LI was born in 1991. He received the bachelor's degree from the Nanjing University of Aeronautics and Astronautics, in 2014, and the master's degree from the Beijing Institute of Technology, in 2015, where he is currently pursuing the Ph.D. degree.

He is currently an Assistant Teacher with the Shandong University of Technology. His research direction is obstacle avoidance algorithm of a snake-like robots based on IB-LBM and APF methods. This algorithm establishes a fluid-solid coupling model between the snake robot and the flow field. The merits of this algorithm is obvious. The complexity of grid division is reduced, the computation speed is accelerated, and the deficiency of the local minimum value of the artificial potential field is solved.

YIRAN WEI was born in Sichuan, in 1993. He is currently pursuing the Ph.D. degree in mechanical and electrical engineering with the School of Mechanical and Electrical Engineering, Beijing Institute of Technology.

He is engaged in the research of control algorithm, aerodynamic analysis, structural design and other aspects related to rotorcraft. At the same time, the control of a snake-like robot is also studied. He mainly engaged in the trajectory tracking control and motion planning of a snake-like robot.

• • •